NASA

Technical Memorandum TM – 86140

MICROWAVE AND X-RAY OBSERVATIONS OF DELAYED BRIGHTENINGS AT SITES REMOTE FROM THE PRIMARY FLARE LOCATIONS

H. Nakajima, B.R. Dennis, P. Hoyng,
G. Nelson, T. Kosugi, K. Kai

AUGUST 1984

National Aeronautics and
Space Administration

Goddard Space Flight Center
Greenbelt, Maryland 20771

MICROWAVE AND X-RAY OBSERVATIONS OF DELAYED BRIGHTENINGS AT SITES REMOTE FROM THE PRIMARY FLARE LOCATIONS

H. Nakajima[1] and B. R. Dennis

Laboratory for Astronomy and Solar Physics

NASA Goddard Space Flight Center

P. Hoyng

Laboratory for Space Research, Utrecht

G. Nelson

CSIRO, Austraila

T. Kosugi and K. Kai

TAO, Tokyo

Received 1984 April 17:

[1] NAS/NRC Resident Research Associate from Nobeyama Solar Radio Observatory of Tokyo Astronomical Observatory

ABSTRACT

We present five examples of solar flares observed with the 17-GHz interferometer at Nobeyama in which a secondary microwave burst occurred at a distance of 10^5 to 10^6 km from the primary flare site. The secondary microwave burst in all five cases had a similar time profile to the primary burst with a delay of 2 to 25 s. The velocity of a triggering agenct inferred from this delay and spatial separation is 10^4 - 10^5 km s^{-1}. The intensity of the secondary burst was a factor of 3 to 25 smaller than that of the primary burst in all events except for one case in which it was a factor of 2 larger. The polarization degree of the secondary burst at 17 GHz was > 35%, significantly higher than the average value for typical impulsive bursts. Two of the events were accompanied by meterwave type III/V bursts located high in the corona between the primary and secondary sites. For two of the other events, X-ray images of the secondary source were obtained with the Hard X-Ray Imaging Spectrometer on the Solar Maximum Mission. A new X-ray source was observed in the region adjacent to the secondary microwave source and was associated with the faint Hα brightenings. No other Hα brightenings were observed at the secondary site for any of the other events.

These observations strongly suggest in each of the five events that the distant microwave burst was produced by electrons with energies of 10 to 100 keV which were channeled along a huge loop from the main flare site to the remote location. In two events, there is evidence that the electron stream from the primary flare site triggered a sympathetic flare within the remote region.

CONTENTS

I. INTRODUCTION

Since the start of routine observations with the 17-GHz solar radio interferometer at Nobeyama in 1978 (Nakajima et al. 1980), it has been noticed that some microwave bursts are accompanied by remote brightenings far away from the primary flare sites. Remote brightenings have also been reported in Hα and in meterwave emissions. They are believed to result from one of two causes: shock waves or fast electrons.

Weak, distant brightenings in Hα emission are known to be caused by the shock wave from an explosive flare. This so-called Moreton wave emanating from the flare site causes progressive, short-lived Hα brightenings of small points in the chromoshere, and the activation of filaments (Svestka 1976). Rust and Webb (1977) suggested on the basis of their analysis of Skylab X-ray data that distant Hα brightenings are caused by slow-mode shocks guided by coronal magnetic loops which can sometimes be seen in soft X-rays. On the other hand, some authors have suggested the possibility of a sympathetic flare being triggered in another active region by a shock wave (Becker 1958; Valnicek 1961; Smith and Harvey 1971) or by energetic particles from the main flare site (Simnett 1974; Gergeley and Erickson 1975). The reality of sympathetic flares is still open to doubt, however, after careful statistical considerations of Hα flare occurrences in different active regions (Svestka 1976).

It has been suggested that distant meterwave and Hα brightnings are caused by the transfer of electrons from the primary to the secondary flare site. Kai (1969) presented some examples of correlated bursts from separated sources observed with the 80 MHz radioheliograph at Culgoora. Successive bursts of similar amplitude were observed to occur from two centers within 10 s of one

another. The initial burst was a normal-drift type III burst and the triggered burst was a reverse-slope (RS) Type III burst, thus suggesting the passage of an electron beam along a large loop. Kai deduced the propagation velocity of 0.3 c similar to that of electrons responsible for type III bursts. Tang and Moore (1982) reported distant Hα brightenings following two large flares, one of which was accompanied by large groups of RS type III bursts. They suggested that the remote Hα brightenings were initiated by the electrons producing the RS burst after they had travelled along the magnetic loops connecting the flare site to the remote patches. Most of the energy to produce the observed Hα bright patches was believed to have followed the electrons in the form of thermal conduction. Recently, Kundu et al. (1983) using the NRAO Very Large Array (VLA), observed a microwave brightening at 5 GHz following a distant subflare. A loop-like structure was also observed at this time stretching $> 10^5$ km from the primary site to the remote bright point. Faint Hα brightenings were also detected simultaneously at the same remote location. They suggested that the Hα distant brightenings were caused by the transfer of electrons with velocities > 6000 km s^{-1} (0.1 keV) originating in the high energy tail of the thermal electron distribution at the primary flare site.

In this paper, we present five examples of distant microwave brightenings at remote regions that were $\sim 1.5 \times 10^5$ to 9×10^5 km from the primary flare site. Our observations suggest (1) that the observed secondary microwave bursts are caused by electron streams with velocities greater than several $\times 10^4$ km s^{-1} (> 10 keV), (2) that the distant microwave burst is closely related to meterwave Type III/V bursts, and (3) that such an energetic-electron stream from the primary flare site is able to trigger a second new flare by an unknown mechanism at the secondary flare site at the footpoint of the huge coronal loop.

II. INSTRUMENTATION

The microwave observations were made with the 17-GHz interferometer at Nobeyama, Japan. The meterwave observations were made with the spectrograph and the radioheliograph at Culgoora, Australia. The X-ray observations were made with the Hard X-ray Burst Spectrometer (HXRBS) and the Hard X-Ray Imaging Spectrometer (HXIS) on the Solar Maximum Mission (SMM).

The 17-GHz interferometer at Nobeyama has been described by Nakajima et al. (1980). It is an east-west one-dimensional interferometer of a multi-correlator type with a compound-type array. The fundamental spacing d_o is 170 cm = 96.4 λ where λ is the wavelength = 1.76 cm. The maximum spacing was 3856 λ (= 40 d_o = 68 m) which corresponds to a spatial resolution of about 40". The spatial resolution was improved to about 20" in July 1981 by installing a new antenna 68 m west of the original westernmost antenna to provide additional Fourier components for spacings every 4 fundamental units (4 d_o) from 44 d_o up to a maximum of 80 d_o compared to the original maximum of 40 d_o (Nakajima et al. 1983). By the inversion of the observed Fourier components, unambiguous east-west profiles of the Sun are obtained for both right- and left-handed circular polarizations with a maximum sampling rate of once every 0.8 s. The accuracy of absolute position determination is estimated to be ± 10". When the profiles are synthesized by applying the Hamming data window used in this study to the observed Fourier components, the estimated sidelobe levels are usually less than a few %.

The radioheliograph at Culgoora has been in routine operation at 40, 80, and 160 MHz (Wild et al. 1967; Sheridan et al. 1973) and at 327 MHz since 1982. The radioheliograph data discussed in this paper consist of two-dimensional images for both circular polarizations at 80, 160, and 327 MHz. The spatial resolutions are 3.75' at 80 MHz, 1.9' at 160 MHz, and 0.95' at 327 MHz, while the time resolution

is 1 s at the maximum sampling rate.

HXRBS provides measurements of the whole Sun X-ray emissions in the energy range from 30 to 500 keV (Orwig et al. 1980). A 15 channel spectrum is obtained every 0.128 s.

HXIS has been described by van Beek et al. (1980). The instrument provides two-dimensional X-ray images of the Sun in the energy range from 3.5 to 30 keV covered in 6 channels. The sensitivity of the instrument is such that only flares with a strong hard X-ray emission are imaged in the two highest energy bands (16-22 and 22-30 keV). The spatial resolution is 8" (FWHM) over a 2'40" fine field of view and 32" over a 6' 24" coarse field of view; the time resolution varies between 1.5 and 7.5 s depending on the mode of operation.

III. OBSERVATIONS

The events showing remote microwave brightenings presented in this paper were selected on the basis of the microwave and X-ray observations. Only events detected between February 1980 and December 1982 were considered and coincident HXRBS and Nobeyama observations were required. The following additional criteria were used to obtain the four selected events:

(1) the peak flux density of the double burst must be $>$ 50 sfu at 17 GHz,

(2) the two components of the double microwave burst must be separated by more than 3 arc minutes in location and by $<$ 1 minute in onset time, and

(3) the time profiles of the two microwave sources must be similar to each other. This last criterion was imposed to reduce the probability of selecting double events that occurred by chance.

A total of 7 events satisfied conditions (1) and (2) for 122 HXRBS and Nobeyama coincident events but only 4 events remained after adding condition (3). A fifth event (the 0200 event on 1980 November 8) was also included although it

did not satisfy criterion #1 above. This was because it occurred only 40 minutes after one of the four selected events and had many similarities with the earlier event.

The general characteristics of the 5 analysed events are summarized in Table 1.

III-1. Properties and Locations of Primary and Secondary Bursts.

Figure 1 shows the east-west brightness distribution at 17 GHz and a sunspot sketch (Solar Geophysical Data) with the possible locations of the two microwave sources for 4 of the analysed events.

In each case the western microwave source was accompanied by an Hα flare (see Table 2), and we denote this as the primary burst. The eastern microwave source was not accompanied by any substantial Hα flare, and we denote this as the secondary burst.

The polarization degree of each of the primary bursts at 17 GHz is similar to the average value for a typical impulsive burst (~ 20%; Kosugi et al. 1983), while the polarization degree of each of the secondary bursts is much higher than this (Table 2).

Although the secondary microwave sources have a simple brightness distribution which is either right- or left-handed polarized, the primary microwave sources have rather complex structures, as shown in the resolution-limited polarization profiles in Figure 1. They have either bipolar structures (the 1980 June 21 and 1981 July 31 events) or they have two sources with the same sense of polarization (the 1982 July 17 event). Note that the primary and secondary sources tend to be oppositely polarized.

The source sizes of the primary and secondary microwave bursts are estimated to be < 20" as a conservative estimation for all events except for the primary burst on 1982 July 17 which had a size of about 35".

Solid arrows in Figure 1 show the positions of the associated Hα flares for all primary bursts and the secondary burst of the 1980 November 8 event (the 0120 event). The Hα positions coincide well with the one-dimensional locations given by the interferometric observations. In the cases where no associated Hα flare was observed, the two-dimensional locations can be determined by taking advantage of the observational fact that the secondary bursts had a small simple structure with the quite high polarization degree. This implies that the secondary bursts were associated with active regions, where the magnetic fields are > a few Gauss, rather than with quiet regions. Then we can identify the active region 16901 as the possible site of the secondary burst of the 1980 June 21 event and the other sunspot area in the active region 18474 as the secondary source on 1982 July 17. (All active regions in this paper are referred to by their Hale number). These candidate source locations are shown by dashed arrows in Figure 1. Each of them is the only active area consistent with the interferometric observations. Although the two dimensional location of the secondary burst on 1981 July 31 can not be determined from this method, the south-east corner of active region 17760 is suggested by the observations with the radioheliograph at Culgoora (see section III-2-(c)). This location is shown also by a dashed arrow in Figure 1.

III-2. Specific Event Observations

a) 1980 June 21

The microwave burst on 1980 June 21 is a strong, multiply impulsive burst. Figure 2 shows the time variations of the peak brightness temperature of the primary and secondary microwave bursts for this event. The time profile corresponding to the difference of right and left circular polarization components is plotted for the secondary component to reduce the effect on the secondary component of

side lobes due to the much stronger primary component. This takes advantage of the characteristic that the polarization degree of the secondary component is much higher than that of the primary component. The overall time profile of the secondary burst is similar to that of the primary burst and shows some correlation in the detailed structure as shown by the arrows.

The overall time profile of the secondary burst is delayed from that of the primary by ~ 7 s. The ratio of the total flux density of the secondary burst to that of the primary is ~ 0.04 at the time of the main impulsive peak and ~ 0.3 during the decay phase.

The dynamic radio spectrum from Culgoora Solar Observatory shown in Figure 3(a) shows that the event was accompanied by strong type III/V bursts followed by a type II burst. The Culgoora radioheliograph images at 80 MHz in Figure 3(b) show that the type III/V sources were significantly elongated parallel to the limb. Other images, not shown, at 40 and 160 MHz and at later times at all three frequencies show that the type III/V sources and the type II source all covered essentially the same area with the same elongated shape. Elongated type II bursts are quite common for limb and behind-the-limb flares and, therefore, may not be significant in terms of a possible link between regions 16898 and 16901. However, the elongated tye III/V sources are unusual. They clearly straddle the two radial lines drawn in Figure 3(b) through regions 16898 and 16901. This may imply that the type V electrons are in high loops connecting the two regions.

b) 1980 November 8

Two double microwave events occurred on this day separated in time by 40 minutes. The first event occurred at ~ 01:20 UT and the second event at ~ 02:00 UT. In both cases the primary source appeared to be in the active region 17244 and the secondary source in the active region 17255. The time profile of the

secondary burst at 17 GHz is very similar to that of the primary in both events as shown later. We designate the first and second events as the 0120 event and the 0200 event, respectively.

SMM was pointing at the secondary flare site and X-ray images obtained with HXIS are available for both of these events. Hα photographs of both regions were obtained from Palehua.

The 0120 Event.

Figures 4(a) and (b) show the time variations of the 17 GHz peak brightness temperature from the primary and from the secondary flare sites, respectively, for this event. The time profile of the 17 GHz secondary burst is very similar to that of the primary with a delay of 25 s.

The HXRBS full sun coverage gives the sum of the 29 - 57 keV X-ray fluxes from the two sites and this is shown in Figure 4(c). The general shape of this time profile is similar to the sum of the primary and secondary microwave time profiles (dashed line in Figure 4(c)) but the ratio of the primary to the secondary X-ray flux appears to be close to unity compared to the value of 0.5 for the ratio of the corresponding microwave fluxes. This suggests that the primary and secondary hard X-ray spectra can be estimated separately from the full disk X-ray data by making use of the time separation. The analysis of the HXRBS data shows that the total hard X-ray spectrum between about 30 and 100 keV is roughly the same at both microwave peak times, suggesting that the primary and secondary hard X-ray spectra are similar.

Figures 4(d) and (e) show the X-ray time profiles for the secondary source obtained from the HXIS data in energy bands from 22 to 30 keV and 3.5 to 5.5 keV, respectively. The optimum signal-to-noise ratio was obtained by summing counts from selected pixels in the HXIS fine and coarse fields of view, from the slits, and from the high energy monitor. The primary flare site was well out of all the HXIS

fields of view so that these time profiles contain little if any contribution from the primary flare. Comparison of these time profiles with the secondary microwave profile shows that the secondary flare begins simultaneously in X-rays and microwaves to within about 10 s.

The soft X-ray fluxes measured by HXIS from 3.5 to 11.5 keV continued to rise gradually even after the microwave main phase at ~ 01:19 - 01:20 UT with a maximum at ~ 01:23:30 UT followed by a gradual decay. From the measured X-ray fluxes in the two HXIS energy bands of 5.5 - 8.0 keV and 8.0 - 11.5 keV, we can calculate the electron temperature (T_e) and emission measure (EM) assuming a homogeneous and isothermal source. We obtain a value of 2.3×10^7 K for T_e and 3.0×10^{47} cm^{-3} for EM at the time of the peak in the soft X-ray flux. An estimate of the volume of the source, $(area)^{3/2}$, can be obtained from the half-power width of the soft X-ray image shown in Figure 5(b). This was estimated to be 7×10^{26} cm^3 giving a value of 4×10^{28} erg for the total thermal energy in the source.

Figure 5(a) shows the Hα flare, the sunspots, the microwave source, and the magnetic neutral line at the primary site (region 17244) in this event. The Hα flare formed two long ribbons located on either side of the magnetic neutral line. They were clearly visible in the picture taken at 01:18:43 UT and lasted for more than 30 minutes. The 17 GHz interferometric observations are consistent with the location of the primary microwave emission being cospatial with the Hα brightening in the positive magnetic field region.

Figure 5(b) shows the spatial relationship of the soft X-ray source, the microwave source, the magnetic neutral line (NASA/Marshall Space Flight Center), the faint Hα brightenings (Palehua Observatory), and the sunspots for the secondary site (Hale region 17255). To align X-ray images with the magnetograms, we used data from the Ultraviolet Spectrometer and Polarimeter also on SMM (UVSP,

Woodgate et al. 1980). UVSP observed a white light sunspot picture after the flare, and therefore, we can overlay the UVSP image and the magnetogram (longitudinal component) by comparing the magnetic intensity map and the UVSP sunspot picture. Next the HXIS and UVSP images can be overlayed by using the known offset between HXIS and UVSP. As UVSP observed also in a high-temperature line (Fe XXI) though it observed only a part of the flaring region, we could improve the accuracy of alinment between the HXIS and UVSP images by overlaying similar feature in both pictures. The accuracy of the alignment for this flare is estimated to be better than about 10".

We can clearly see a soft X-ray source in the central part of Figure 5(b). This soft X-ray source is located across the magnetic neutral line and has a projected length of about 1'. Images in harder X-rays from 11.5 to 30 keV show a similar source at the same location although the image quality is poor due to the low counting rate. The secondary microwave source corresponds to the westernmost end of the soft X-ray source, which coincides with a small sunspot with negative magnetic polarity. The polarization sense (left hand) of the microwave source agrees with the sign (-) of the associated magnetic field assuming that 17 GHz microwaves are emitted in the extraordinary mode. The Hα patrol film from Palehua Observatory shows two faint, compact Hα brightenings associated with the two ends of the soft X-ray source. These photographs taken every minute show that the brightenings appeared at 01:19:13 UT, reached maximum at 01:20:13 UT, and then decayed gradually for ~ 15 minutes.

Some weak enhancements were already seen before the onset time of the 0120 event. Very weak Hα brightenings were observed as early as 01:15:43 UT at the primary site. The HXIS soft X-ray images of the secondary site show that a weak, elongated structure was already present at this time along the same magnetic neutral line.

We can also see in Figure 5(b) a huge X-ray structure imaged in the HXIS coarse field of view. This source extended over the solar limb high above the soft X-ray source in Hale region 17255. This huge X-ray structure may be a remnant of the gigantic loop observed with HXIS on 1980 November 6 and 7 and reported by Svestka et al. (1983). Alternatively, it may have been part of a loop which was newly excited before our microwave event. This structure was stationary and could be seen before the occurrence of the 0120 event and was still present after the 0200 event. We could not find any correlation between this loop and the secondary X-ray source.

The 0200 Event

Figure 6 shows time variations of the 17 GHz peak brightness temperature from the primary and secondary sites, the soft X-ray flux measured with HXIS from the secondary site, and the full disk hard X-ray flux measured with HXRBS. The time profile of the secondary burst at 17 GHz is similar to that of the primary. Some correlation between the features in the primary and secondary time profiles is shown by the arrows in Figure 6. The delay time of the secondary time profile with respect to the primary is 11 s.

The HXRBS time profile has peaks labelled 1 and 2 in Figure 6(c) which coincide with the primary and secondary microwave peaks, respectively. The soft X-ray emission from the secondary site began to increase at the time of the peak from the secondary microwave source and peaked about 1 minute later.

The HXRBS time profile showed an earlier weak enhancement from 01:57:50 to 01:58:15 UT that was accompanied by an Hα subflare in region 17255 as reported from Palehua Observatory. This subflare was located from 1' to 2' south-west of the secondary Hα brightenings of the 0120 event. A very weak 17 GHz microwave burst was observed at this time at a location consistent with the south-western

part of the Hα subflare. As we can not find any clear relationship between the event at ~ 01:58 UT and our double burst at 02:00 UT, we will not discuss this subflare any further.

Figure 7(a) shows that the primary Hα flare of the 0200 event occurred slightly to the south of the primary Hα flare of the 0120 event. Several bright features were visible on both sides of the magnetic neutral line. The location of the primary microwave emission is consistent with that of the brightest Hα feature in the positive magnetic field region.

Figure 7(b) shows the spatial relationship of the soft X-ray source, the microwave source, the magnetic neutral line (Marshall Space Flight Center), the faint Hα brightening, and the sunspots for the secondary site of the 0200 event. Although the soft X-ray source at the secondary site was smaller in extent than the secondary X-ray source of the 0120 event, it was located at almost the same place across the magnetic neutral line. The secondary microwave source corresponds to the western end of the soft X-ray source above the sunspot with negative magnetic polarity. The Hα patrol film from Palehua Observatory shows that a faint Hα brightening occurred at the eastern end of the secondary X-ray source, near the location of the eastern Hα brightening at the secondary site of the 0120 event. This brightening appeared in the picture taken at 01:58:13 UT, reached a maximum in the next picture taken one minute later, and then decayed rapidly.

The whole story described above shows that the 0120 and 0200 events were almost homologous at both the primary and secondary sites.

c) 1981 July 31

The microwave burst on 1981 July 31 is a strong, multiply impulsive burst. Figure 8 shows the time variations of the peak brightness temperature of the primary and secondary microwave bursts for this event. Also shown is the time

variation of the source position of the primary burst. The primary and secondary time profiles show remarkable similarities in the detailed structure. The secondary burst is delayed with respect to the primary burst by 1.7 s. The intensity ratio of the secondary burst to the primary one is 0.1 to 0.2. As shown in figure 8(c), the source of the primary microwave emission is at slightly different locations for the individual peaks.

Figure 9 shows the dynamic spectra and the radioheliograph images from Culgoora Solar Observatory. The event was accompained by a strong type III/V burst, followed by a type II burst. From the start of the Type III/V burst at ≈ 00:51 UT a double source at 160 MHz was observed at positions labelled 1 and 2 in Figure 9(b). As the burst progressed, the inner source 2 moved lower in height to the location labelled 3 but the outer source labelled 1 stayed fixed. The Culgoora spectrograph shows that the second microwave burst beginning at ≈ 00:53 UT was accompanied by a decimeter burst with pulsations which extend down to 160 MHz and gave rise to a new double source at position 1 and 4 (the component at position 1 extended to position 2).

The flare related sources (1, 2, 3, and 4) are clearly very high in the corona above the flaring region and need to be projected downwards before they can be associated with a particular region. The two radial lines in Figure 9(b) are drawn through the primary Hα flare site marked with an 'X' and the sunspot group (dotted circle) in the south-east corner of region 17760. Then, the sources 1 and 2 are located above the primary Hα flare site and the source 4 is located above the sunspot group which is then a candidate for the secondary microwave site. This location is consistent with the possible positions of the secondary microwave source at 17 GHz (see Figure 1(c)). The slightly elongated source 3 straddles both radial lines. These observations suggest that the emission from the sources 3 and 4 and probably 2 are due to type V electrons which are

trapped around the top of the huge loops connecting the primary and secondary microwave sites, while the emission from source 1 may be due to type III electons traveling along open field lines.

d) 1982 July 17

The microwave burst on 1982 July 17 peaked at 1370 sfu at 17 GHz and hence is classified as a great burst with a rather gradual time profile. Figure 10 shows the time variations of the peak brightness temperature of the primary and secondary microwave bursts for this event. The overall time profile of the secondary burst is similar to that of the primary although it is disturbed by sidelobes due to the strong primary burst. In this case it is difficult to assess unambiguously the time delay of the secondary burst, but inspection of the figure suggests a delay of 8 ± 5 s. The intensity ratio of the secondary burst to the primary one is about 0.04.

During the flare, this event was accompanied by a decimetric type I burst which occurred exactly over the primary Hα flare location but was accompanied by almost no meterwave activity. The absence of any radio emission at frequencies below 300 MHz during the flare implies that the energetic electrons were confined to altitudes less than 2×10^5 km. Assuming a semicircular loop, this implies a spatial separation between the primary and secondary sites of less than 4×10^5 km, and supports the conclusion reached in section III-1 that both sites are contained within active region 18744.

IV SUMMARY OF OBSERVATIONS

We have presented observations of 5 microwave bursts in which a secondary burst occurred at a location far away from the primary flare site. The main results of these observations are summarized below:

(1) The distance along the solar surface between the primary and secondary sites,

the time delay of the secondary microwave burst with respect to the primary one, and the deduced velocity of the triggering agent are given in Table 3 for each event. The weak positive correlation between the distance and time delay supports the idea that the double events are physically connected and not just the result of chance coincidences.

(2) The secondary site is located to the west of the primary site for all of the events. This may be related to the strucrure of the active regions.

(3) The peak primary flux was greater than the peak secondary flux for all of the events except for the 0120 event on 1980 November 8 when the primary was a factor of two smaller than the secondary. The secondary to primary ratios for all events are given in Table 2.

(4) The polarization degree of the secondary burst at 17 GHz is high (> 80% for some events) compared to the average value of ~ 20% for typical impulsive bursts. Also, the primary and secondary sources tend to be oppositely polarized.

(5) The secondary burst is not accompanied by any substantial Hα brightenings. Even the secondary sites of the November 8 events, where new flares were excited, were accompanied by only very weak Hα brightenings that were not even classified as subflares.

(6) Two of the double microwave bursts were accompanied by type III/V bursts which were located high in the corona between the primary and secondary microwave sites.

Simultaneous observations with HXIS and HXRBS give the following observational results for the 0120 event on 1980 November 8.

(7) A new X-ray source occurred in the region adjacent to the secondary microwave source. The X-ray source was associated with faint, compact Hα brightenings at its eastern and western ends.

(8) The flare at the secondary site began simultaneously in X-rays and microwaves to within 10 s.

(9) The time profile of the X-rays (≥ 10 keV) from the secondary site was similar to that of the secondary microwave burst in starting time and duration.

(10) The maximum energy of the hard X-ray emissions from the secondary X-ray source was at least several tens of keV.

(11) It is suggested that the secondary X-ray spectrum was roughly the same as the corresponding primary X-ray spectrum at energies between 30 and 100 keV.

(12) A weak soft X-ray source at the secondary site was observed with a faint Hα enhancement at the primary site well before the main phase.

V. INTERPRETATION

The existence of the time delay between the primary and secondary burst and the fact that the primary microwave bursts are associated with more intense Hα flares than the corresponding secondary bursts, strongly suggest that the secondary burst was excited by an agent from the primary burst site. The velocity required by the measured time delay and spatial separation imply that the agent that excited the secondary burst must be high energy electrons produced in the primary flare site. The similarity found between the primary and secondary microwave time profiles also support this point of view. We suggest that high energy electrons escaping from the primary site are channeled along a huge coronal loop connecting the primary site with the secondary site and stream down

to the remote footpoint to trigger the secondary microwave burst. This suggestion is also supported by the observation that the primary and secondary microwave sources are oppositely polarized in all cases except for the limb event on 1980 June 21. The association of the elongated type V sources with our microwave events shows evidence for such huge coronal loops. A fraction of the electrons which cause the type III bursts may be trapped in the huge loop high in the corona and become visible as a type V burst through the generation of plasma waves (Weiss and Stewart 1965).

The secondary microwave emission comes from the low-coronal part of the footpoint of the huge loop. This is shown by the fact that the secondary microwave source is highly polarized and has a size of less than 20".

The velocities of the electrons that excite the secondary microwave bursts must be higher than the velocities listed in Table 3 that were calculated assuming that the triggering agent travelled along the surface between the primary and secondary sites. We consider that the electrons were guided along huge coronal loops. If we assume that the loops were semicircular and the electron pitch-angles were 0", the calculated electron velocities range from 5×10^4 km s^{-1} to 1.8×10^5 km s^{-1} and the corresponding energies are given in Table 3. The calculated electron velocities would be somewhat larger for non-zero pitch angles but we do not believe that the average pitch angle can be very large. This is because the strength of the magnetic field at the top of the coronal loop is surely much less than the strength of the field at the footpoints. Consequently, any electron injected into the loop near one footpoint with a large pitch angle will necessarily have a small pitch angle at the top of the loop. Even assuming an average pitch angle of 45° would only increase the electron velocity by $\sim$ 40%. The derived velocities are higher than the velocity ($>$ 6000 km s^{-1}) derived from the VLA observations (Kundu et al. 1983), while they are similar to the 10^5 km s^{-1}

velocities obtained by Kai (1969) and Tang and Moore (1982).

The secondary microwave bursts that we have observed may be different from the events observed by Kundu et al. (1983) or by Tang and Moore (1982). The secondary microwave burst observed by Kundu et al. was accompanied by Hα brightenings and occurred in a rather uniform magnetic field region. Furthermore, it was not polarized. The remote Hα brightenings observed by Tang and Moore occurred in quiet regions. These observations imply weak magnetic fields. On the other hand, our secondary microwave bursts were highly polarized and must have occurred in stronger magnetic field regions near sunspots.

This point of view is consistent with the absence of Hα flares at the secondary sites as can be seen from the following argument. The flux density, F, of an optically-thin microwave source with a nonthermal electron distribution is related to the magnetic field strength, B, the density of high energy electrons, N, and the volume, V, by the following simplified expression given by Dulk and Marsh (1982):

$$F \propto N V B^{0.90\delta - 0.22},$$

where δ is the power-law index of the electron spectrum. As δ is estimated to be between 3 and 7 from the hard X-ray spectra for our events, the microwave emission at 17 GHz (which is usually optically thin) depends more strongly on the magnetic field strength than on the total number of high energy electrons. Therefore, we can expect substantial microwave emission at 17 GHz from stronger magnetic field regions near sunspots, even though there are not enough high energy electrons streaming into the secondary site to cause Hα brightenings.

The association of the type III/V bursts with our microwave events also supports the point of view that both the primary and secondary bursts occur in regions with strong magnetic fields. If the huge coronal loop were rooted in an active region with strong magnetic fields at the primary site and in a quiet

region with weak magnetic fields at the secondary site, it is unlikely that enough type III electrons could be trapped in such an asymmetric loop to produce a type V burst.

All of the above considerations lead us to suggest the model of our double microwave bursts, shown schematically in Figure 11. Most of the high energy electrons escaping from the primary site towards the secondary site along the huge coronal loop are trapped around the top part of the loop causing the type V burst. The remaining electrons precipitate into the secondary site, causing the microwave burst in the low corona.

High energy electrons impinging on the low corona and the chromosphere at the secondary site heat the chromosphere and cause Hα brightenings. However, the secondary site of the June 21 event was not accompained by any Hα subflare. The November 8 secondary sites were accompained only by very faint Hα brightenings. We have no detailed Hα information for the remaining events. We believe that the observed secondary Hα brightenings and X-ray emissions in the November 8 events were not produced directly by the fast electrons impinging on the footpoint of the huge loop. Rather we believe that they resulted from newly excited flares at the secondary sites (see later discussion). Consequently, it is possible that any Hα brightenings resulting from the electrons from the primary site may be much weaker. These considerations allow us to estimate the energy deposited in the secondary site by electrons from the primary source for both the June 21 event and two events on November 8.

The thermal energy content in the chromosphere, where the core of the Hα is formed, is of the order of 10^8 erg cm^{-2}, and the total radiative loss rate is of the order of 10^6 erg cm^{-2} s^{-1} (Athay 1976). If we assume that a subflare occurs when the thermal energy of the chromosphere is increased by a factor of 10, then we get the following equation relating P, τ, and S.

$$(P_2 - 10^6\ S)\ \tau\ < 10^9\ S, \qquad (1)$$

where, P_2 is the total energy streaming into the secondary site during τ, and S is the area of the secondary site into which electrons stream from the primary site. For both events, we get $S < 2\times10^{18}$ cm^2 from the interferometric observations and $\tau \leq 70$s from the half-width duration of the microwave bursts. This implies that

$$P_2\tau < 2\times10^{27} \text{ erg}. \qquad (2)$$

Next, we estimate the ratio of the power deposited by electrons that stream into the secondary site to the power deposited by electrons at the primary site for the 1980 June 21 event and for the two events on 1980 November 8. This ratio can be obtained from inequality (2) and from the spectrum of hard X-rays from the primary site. Here, we assume that the hard X-ray spectrum from the primary site is roughly equal to that from the full disk. This is because the secondary hard X-ray flux is probably much smaller than the primary for the 1980 November 8 (0200 event) and for the 1980 June 21 event as expected from the microwave flux ratio. Also the hard X-ray spectrum of the 1980 November 8 event (0120 event) in Table 1 is obtained at the peak time of the primary microwave burst when the X-ray flux from the primary site is probably much larger than that from the secondary site.

We assume that the power-law electron spectra at the primary site can be derived from the corresponding hard X-ray spectra under the thick target assumption (Brown 1971). The observed hard X-ray spectrum at 1 AU from the primary site is given by

$$I_1(\varepsilon) = a\varepsilon^{-\gamma} \text{ photons } (\text{cm}^2\ \text{s keV})^{-1}, \qquad (3)$$

where ε is the photon energy in keV, and a and γ are found in Table 1. Applying standard thick target calculations (Brown 1971), the power deposited by electrons with energies larger than E is:

$$P_1(>E) = 4.2\times10^{24}\ a\ \gamma\ (\gamma-1)\ B(\gamma-1/2,\ 1/2)\ E^{-\gamma+1} \text{ erg s}^{-1}, \qquad (4)$$

where E is in keV. A small fraction of this power streams into the secondary target. Only electrons with $E > E^*$ can go all the way to the secondary target without losing all of their energy in Coulomb collisions with the ambient plasma in the loop connecting the primary and secondary sites. Hence, we assume that the total power P_2 deposited in the secondary target is given by

$$P_2 = \eta\, P_1(>E^*) \quad \text{erg s}^{-1} , \tag{5}$$

where η is a constant of proportionality. The values of E^* for the June 21 and November 8 events given in Table 4 were obtained by assuming that the loop was semicircular with a density 10 times the normal coronal density (Allen 1976).

By combining Equation (5) with Equation (2) we find that

$$\eta < 2\times10^{27}/\tau P_1(>E^*).$$

Upper limits on η obtained in this way are given in Table 4. They indicate that the total power deposited by electrons that stream into the secondary site was < 1% of the power deposited by electrons with energies larger than E^* at the primary site for each of the three events.

It was observed for the November 8 events that the secondary X-ray sources extended across the neutral line. This we interpret as indicating a new small loop excited in the region adjacent to the secondary microwave source. This new X-ray loop was associated with faint, compact Hα brightenings at its footpoints. The flare at the secondary site begins almost simultaneously in X-rays and microwaves. These observational facts lead to the following two possible interpretations of the November 8 events:

One interpretation is that a new flare (a sympathetic flare) was triggered at the secondary site by an electron stream from the primary site. Electrons must have been accelerated or heated to at least several tens of keV in this sympathetic flare because X-rays between 29 and 57 keV were observed corresponding to the secondary microwave burst as shown in Figure 4.

The other interpretation is that some of the fast electrons precipitating into the thick target at the footpoint of the huge loop at the secondary site were transferred into the small loop adjacent to the huge loop through some processes such as scattering or drifting, and were trapped. If this were the case, we would expect that most of the X-rays from the secondary site would come from the thick target at the footpoint of the huge loop because only a small number of the electrons entering the footpoint of the huge loop would be transferred to the adjacent small loop. The footpoint of the huge loop at the secondary site is located in the negative magnetic field region as suggested by the polarization sense of the secondary microwave source. Our observations clearly show in Figures 5 and 7 that most of the X-rays come from the small loop and only weak X-ray emissions come from the negative magnetic field region where the footpoint of the huge loop is considereed to be located. Therefore, this interpretation can not be correct.

Thus, we have strong evidence that a sympathetic flare can be triggered by a high energy electron stream from a distant main flare site. The reality of the connection between the two active regions on 1980 November 8 is based mainly on the observations that the time profiles of the primary and secondary microwave bursts were very similar and that a second double event occurred some 40 minutes after the first. Dennis et al. (1984) have also suggested that an electron beam can trigger a sympathetic flare based on observed coincidences of reverse slope type III bursts, hard X-ray spikes, and subsequent normal slope type III bursts.

The observations of the bursts on 1980 November 8 give information on the mechanism by which a sympathetic flare may be generated. A weak soft X-ray source at the secondary site was already observed with a faint Hα enhancement at the primary site well before the onset time of the main phase of the 0120

event on 1980 November 8. Furthermore, the time profile of hard X-rays (> 10 keV) from the sympathetic flare was similar to that of the primary microwave burst. If the sympathetic flare was due to the onset of a catastrophic instability which is triggered by a high energy electron stream, we would expect that the time scale and intensity of the flare would not depend on the time scale and intensity of the electron stream that triggered it but rather on the type of instability and on the amount of free energy available at the secondary site. Rather, the above observational facts suggest that the sympathetic flare is due to a flare instability which works as an amplification mechanism - i.e., the number of electrons that are accelerated or heated in the sympathetic flare is proportional to the number of high energy electrons streaming in from the primary flare site. The efficiency of the energy amplification in this mechanism is greater than one order because the total energy of electrons streaming into the secondary site is estimated to be $< 2 \times 10^{27}$ erg and the total thermal energy in the second new flare is $\sim 4 \times 10^{28}$ erg for the 0120 event on 1980 November 8.

VI. CONCLUDING REMARKS

The present observations have indicated that well separated active centers on the Sun can interact with one another through huge coronal loops connecting them. High energy electrons from the primary flare site can travel vast distances along the loops and excite a second microwave burst in the remote region at the other footpoint of the loops. Sometimes such high energy electrons from the primary flare site can trigger a new flare (a sympathetic flare) in a small loop adjacent to the secondary footpoint of the huge coronal loops. The latter observational result implies that if a flare occurs in any one of many adjacent loops in an active region, it can trigger the successive firings of all the adjacent loops resulting in the flaring of the whole region almost simultaneously. This may be an important clue to the flare trigger mechanism.

ACKNOWLEDGEMENTS

We would like to thank R.A. Shine from UVSP for supplying us with the UVSP data and helping us to overlay the HXIS images and the magnetogram. Also we are grateful to M. Hagyard from Marshall Space Flight Center for the magnetograms of the November 8 flare and V. Miller from National Geophysical Data Center for the high-quality Hα film of the November 8 flare. We also thank G.S. Kennard for helping with the data reduction and G. Wharen for typing the manuscript.

This research was carried out while one of us, H. Nakajima, was staying at the Laboratory for Astronomy and Solar Physics of the NASA Goddard Space Flight Center as a research associate of the NAS/National Research Council on leave from Nobeyama Solar Radio Observatory of TAO. The hospitality of K.J. Frost, SMM project scientist, and his colleagues is gratefully acknowledged. H. Nakajima also expresses special thanks to his colleagues at the Nobeyama Solar Radio Observatory.

TABLE 1

CHARACTERISTICS OF ANALYSED EVENTS

A. Microwave and Hard X-Ray Emission

Date	17 GHz Start (UT)	Peak (UT)	Duration (min.)	Peak flux (sfu)	X-Ray Spectrum $30<\varepsilon<500$ keV (photons $cm^{-2}s^{-1}keV^{-1}$)
1980 June 21	0117.3	0118.7	3.3	2000	$9 \times 10^4\ \varepsilon^{-2.0}$
1980 November 8					
0120 event	0118.5	0119.5	3.0	81	$5 \times 10^8\ \varepsilon^{-6.0}$
0200 event	0158.2	0158.7	3.0	20	$1 \times 10^7\ \varepsilon^{-5.0}$
1981 July 31	0051.1	0053.3	3.2	210	$4 \times 10^6\ \varepsilon^{-4.1}$
1982 July 17	0203.5	0205.9	5.0	1370	$7 \times 10^8\ \varepsilon^{-4.9}$

B. Metric and Decimetric Emission

Date	Decimetric Start (UT)	End (UT)	Intensity	Metric Start (UT)	End (UT)	Intensity	Type
1980 June 21				0111	0135		IV
	0118.5	0120.5	2	0117	0119.5	2	IIIG, V
	0119	0126.6	1	0120	0138	2	II
1980 Nov 8							
0120 event	No activity			No activity			
0200 event	No activity			No activity			
1981 July 31				0050.2	0101.4	3	V
	0050.5	0056	1	0050.5	0100	3	IIIGG, V
				0050.8	0112.3	2	II
	0052	0057	1				IV, P
1982 July 17	0203.5	0209.0	2				IS, C

TABLE 2

CHARACTERISTICS OF PRIMARY AND SECONDARY FLARES

Date	Hα Flare		Polarization at 17 GHz		Flux Ratio
	Primary	Secondary	Primary (%)	Secondary (%)	(secondary/primary)
1980 June 21	1B(N19W90)	no brightening*	< 10	~ 50	0.04 - 0.3
1980 November 8					
0120 event	-N(N10W20)	?F(S10E50)	~ 25	~ 35	2
0220 event	-N(N10W18)	?F(S10E50)**	~ 30	~ 70	0.15
1981 July 31	-N(S08W46)	non reported	~ 15	> 80	0.1 - 0.2
1982 July 17	1B(N11W33)	non reported	~ 10	> 80	0.04

* M. McCabe 1982, private communication.

** based on the patrol film from Palehua Observatory.

TABLE 3

VELOCITIES OF TRIGGERING AGENT

Date	Distance along surface (10^5 km)	Time Delay (s)	Trigger Velocity along surface (10^4 km s^{-1})	Required* Electron Energy (keV)
1980 June 21	3.8	7	5	19
1980 Nov 8				
0120 event	8.9	25	4	7
0200 event	8.6	11	8	40
1981 July 31	1.9	1.7	11	120
1982 July 17	1.5	8 ± 5	3 ± 2	8 ± 6

* The electron energy was calculated assuming propagation along a semicircular loop with zero pitch angle.

TABLE 4

RATIO OF SECONDARY TO PRIMARY ENERGY DEPOSITION

Date	Primary Site		η	E*	τ
	Electrons(>E*) (electrons s^{-1})	Energy(>E*) (erg s^{-1})		(keV)	(s)
1980 June 21	1.8×10^{36}	8.1×10^{28}	$< 4 \times 10^{-4}$	15	68
1980 Nov. 8 0120 event	3.8×10^{35}	1.5×10^{27}	$< 4 \times 10^{-3}$	20	34
0200 event	1.5×10^{34}	6.1×10^{27}	$< 1 \times 10^{-2}$	20	30
1981 July 31	1.9×10^{36}	5.6×10^{28}	-	14	35
1982 July 17	5.6×10^{37}	1.6×10^{29}	-	14	104

E* - minimum energy of an electron required to traverse a semicircular coronal loop joining the primary and secondary sites.

η - ratio of the power deposited by electrons streaming into the secondary site to the power deposited at the primary site.

τ - duration of the interval that electrons are streaming into the secondary site.

REFERENCES

Allen, C. E. 1976, Astrophysical Quantities, Third Edition (London: University of London), p. 177.

Athay, R.G. 1976, The Solar Chromosphere and Corona, Quiet Sun (Dordrecht, Holland: D. Reidel Pub. Co.), p. 384.

Becker, U. 1958, Z. Astrophys., 44, 243.

Brown, J.S. 1971, Solar Phys., 18, 489.

Coffey, H.E. 1983, Solar Geophysical Data, No. 467, Part II, p. 38. (Boulder: U.S. Department of Commerce).

Dennis, B.R., Benz, A.O., Ranieri, M., and Simnett, G.M. 1984, Solar Phys., 90, 383.

Dulk, G.A. and Marsh, K.A. 1982, Astrophys. J., 259, 350.

Gergely, T.E. and Erickson, W.C. 1975, Solar Phys., 42, 467.

Kai, K. 1969, Proc. Astron. Soc. Australia, 1, 186.

Kosugi, T., Kai, K., and Suzuki, T. 1983, Solar Phys., 87, 373.

Kundu, M.R., Rust, D.M., and Bobrowsky, M. 1983, Astrophys. J., 265, 1084.

McCabe, M. 1982, private communication.

Nakajima, H., et. al. 1980, Publ. Astron. Soc. Japan, 32, 639.

Nakajima, H., Sekiguchi, H., Kosugi, T., Shiomi, Y., Sawa, M., Kawashima, S., Hashimoto, K., and Kai, K. 1983, Publ. Astron. Soc. Japan, submitted.

Orwig, L.E., Frost, K.J., and Dennis, B.R. 1980, Solar Phys., 65, 25.

Rust, D. and Webb, D. 1977, Solar Phys. 54, 403.

Sheridan, K.V., Labrum, N.R., and Payton, W.J. 1973, Proc. IEEE, 61, 1312.

Simnett, G.M. 1974, Solar Phys., 34, 377.

Smith, S.F. and Harvey, K.L. 1971, in Physics of the Solar Corona, ed. C.J. Macris (Dordrecht, Holland: D. Reidel Publ. Co.), p. 156.

Svestka, Z. 1976, Solar Flares (Dordrecht, Holland: D. Reidel Publ. Co.) p. 225.

Svestka, Z., et. al. 1983, Solar Phys., 85, 313.

Tang, F. and Moore, R.L. 1982, Solar Phys., 77, 263.

Valnicek, B. 1961, Bull. Astron. Inst. Czech., 13, 91.

Van Beek, H.F., Hoyng, P., Lafleur, B., and Simnett, G.M. 1980, Solar Phys., 65, 39.

Weis, A.A. and Stewart, R.T. 1965, Australian J. Phys., 18, 143.

Wild, J.P. 1967, Pro. Inst. Radio Electron. Eng. (Aust.), 28, 277.

Woodgate, B.E., et. al. 1980, Solar Phys., 65, 73.

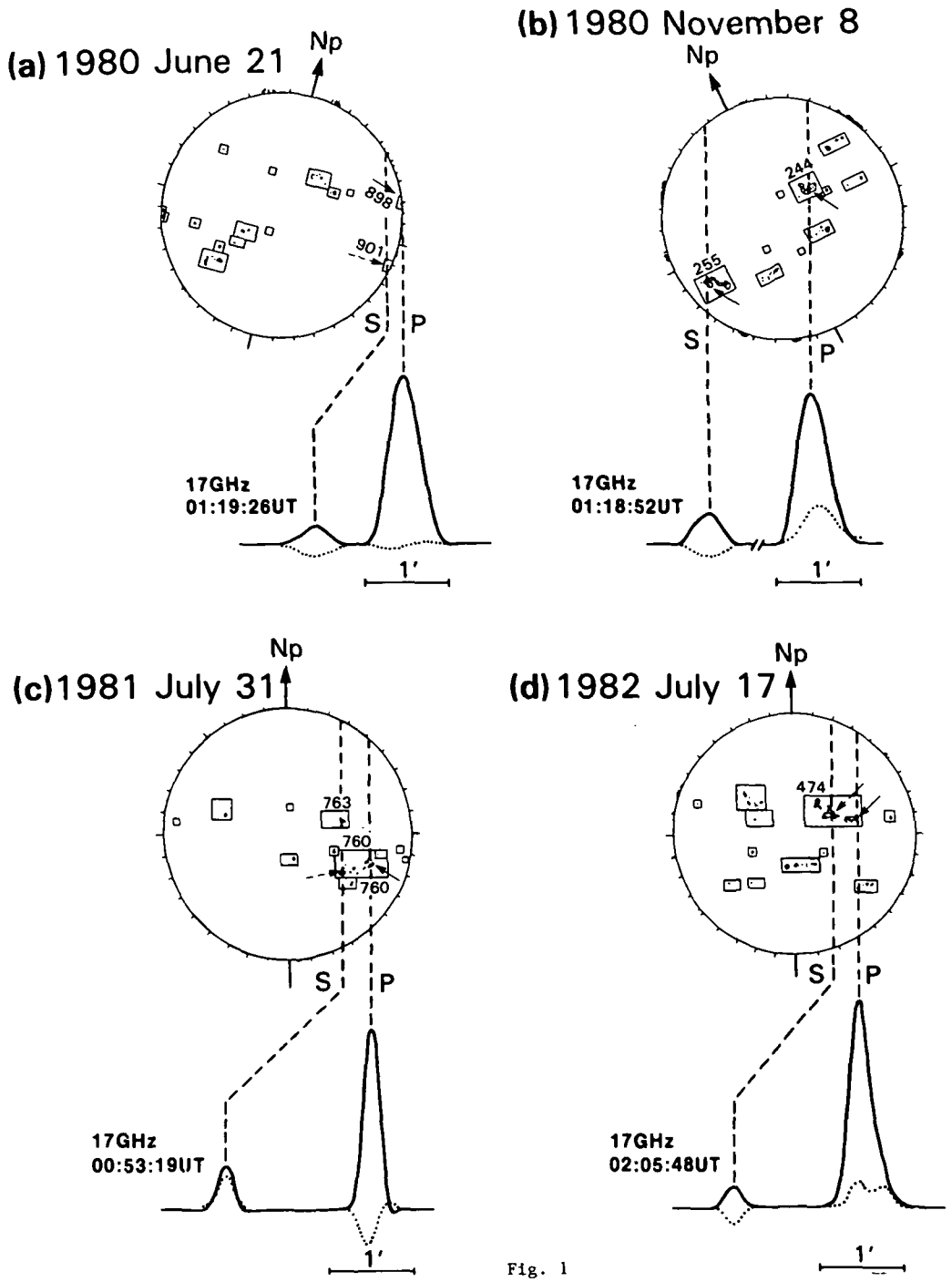

Figure 1. Combined pictures of east-west brightness distributions at 17 GHz and sunspot sketches from Solar Geophysical Data for the 4 analysed events. Both the total intensity profile (solid line, R+L) and the polarization profile (dotted line, R-L) are presented. The solid arrows indicate the positions of Hα flares or brightenings. The dashed arrows indicate possible candidates for the secondary microwave sites. The lines marked P and S indicate the possible locations of the primary and secondary microwave bursts, respectively.

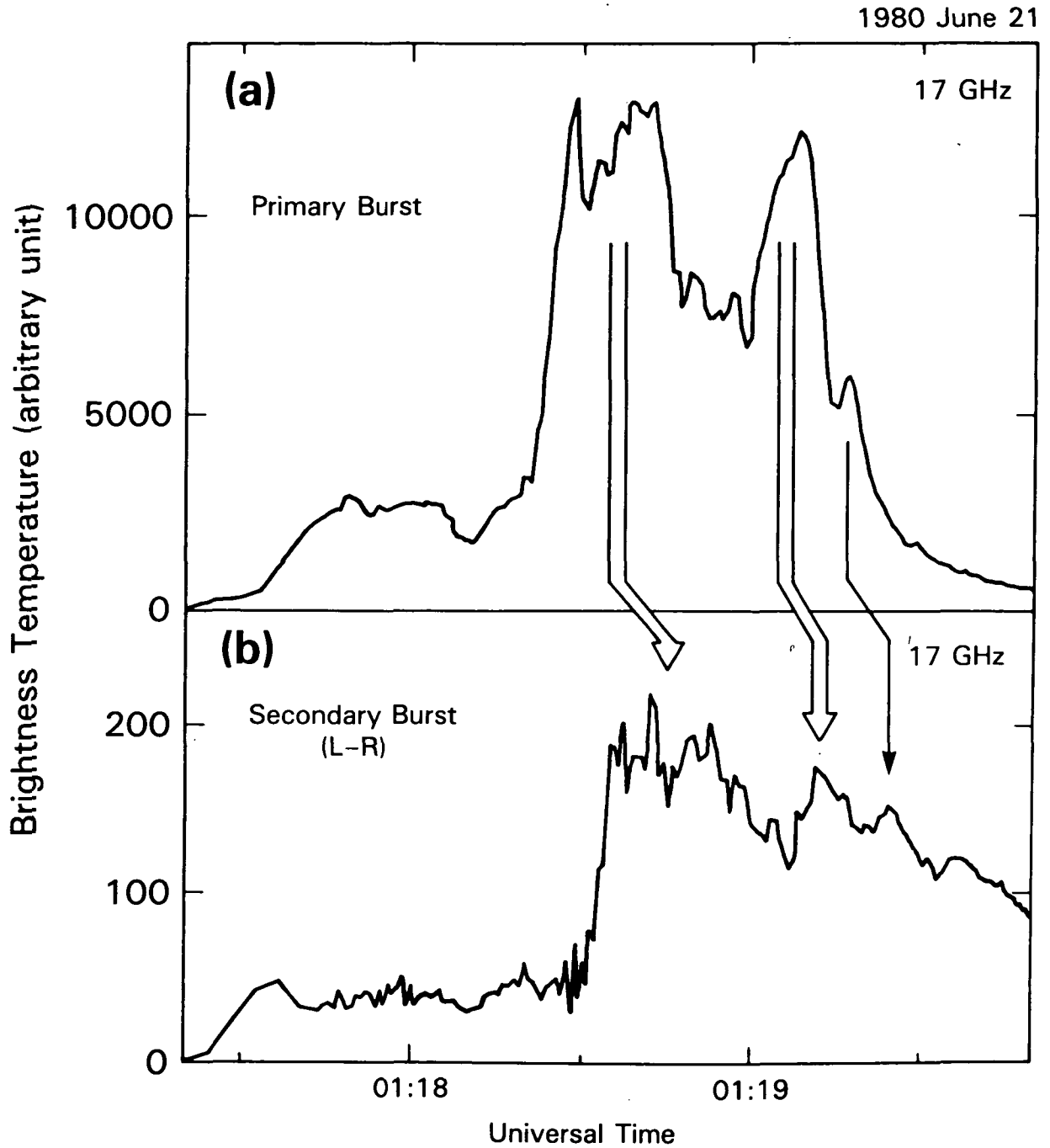

Figure 2. Time variations of the peak brightness temperature of the primary and secondary bursts of the 1980 June 21 event. Note that the polarization profile (the difference of right and left circular polarization components, R–L) is used in place of the total intensity profile (R+L) only for the secondary component of this event. Although the peak brightness temperature is scaled in arbitrary units, the relative ratio is correct between the primary and secondary time profiles for individual events. Arrows indicate well-defined peaks in the primary burst that appear to correspond to delayed peaks in the secondary burst.

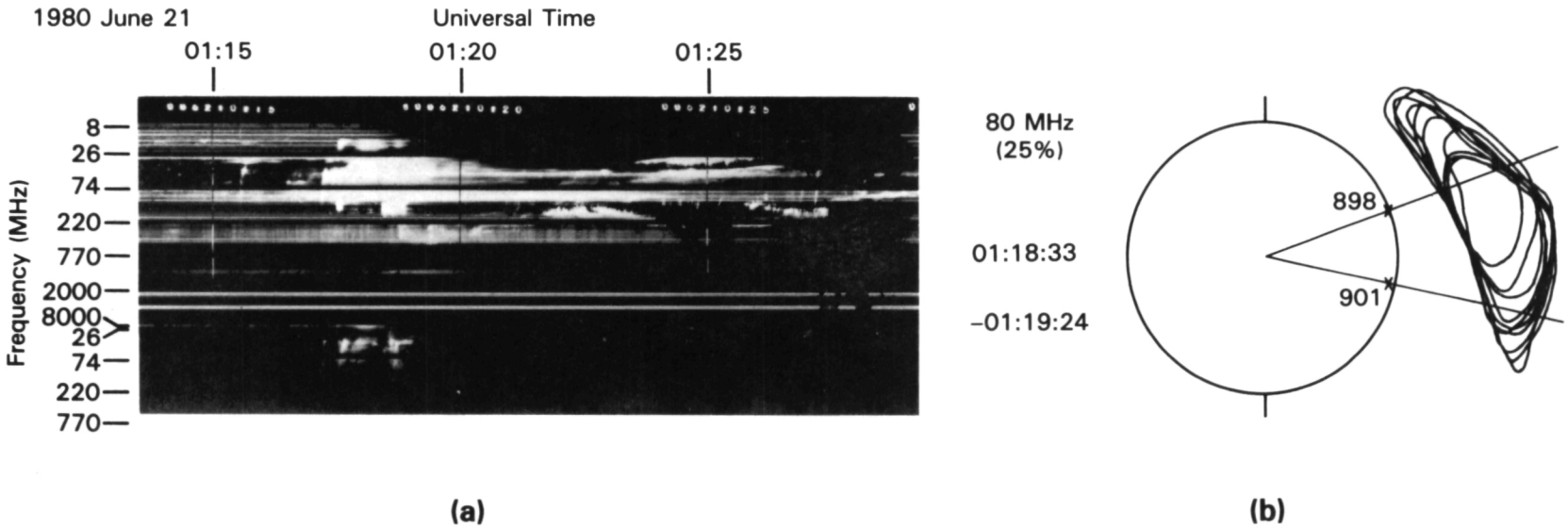

Figure 3. (a) Dynamic radio spectrum showing the intensity as a function of time for frequencies from 8 MHz to 8 GHz. The bottom part of the plot covers the frequency range from 26 to 770 MHz with reduced intensity. (b) Radio heliograph images at 80 MHz showing the 25% contours of the type III/V sources at times between 01:18:33 and 01:19:24 UT. Two radial lines are drawn through active regions 16898 and 16901.

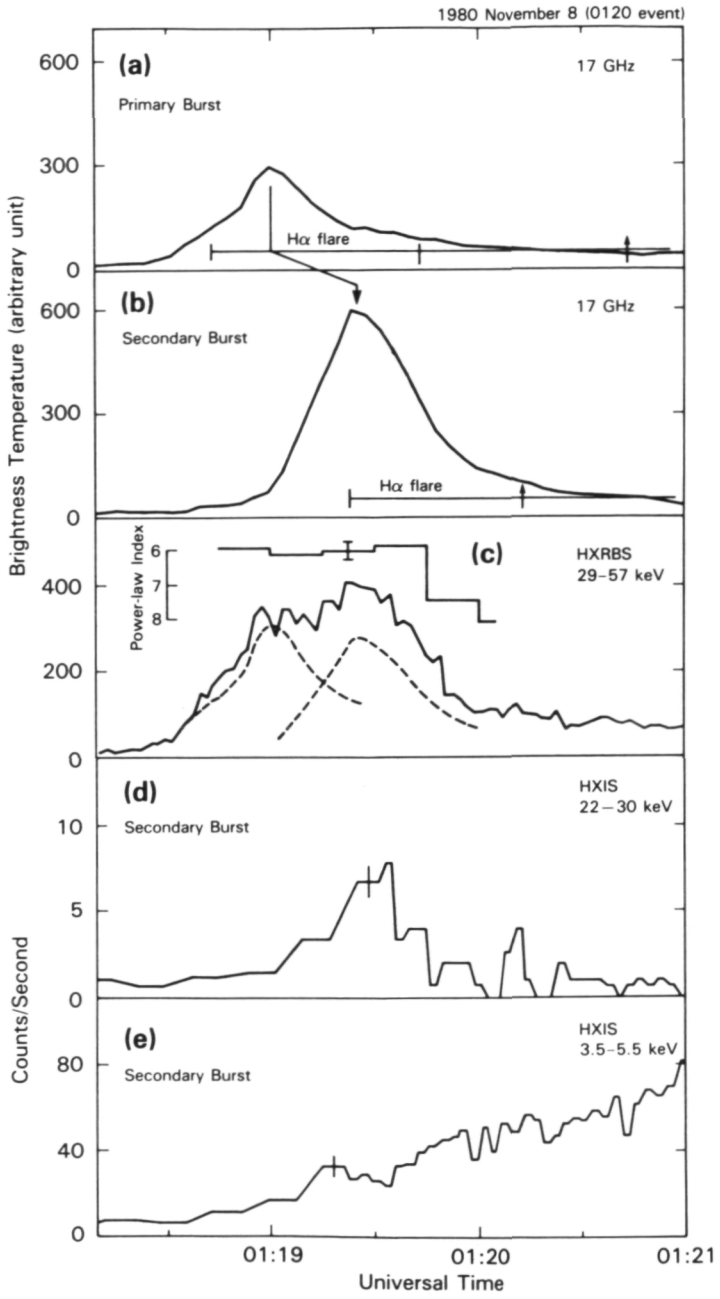

Figure 4. Time variations of the microwave and X-rays in different energy bands from the primary and secondary site of the 0120 event on 1980 November 8. The 3.5-5.5 and 22-30 keV X-ray time profiles were obtained with HXIS. The 29-57 keV X-ray time profiles (dashed line) from the primary and secondary sites were obtained from X-ray data (solid line) integrated over the whole disk from HXRBS by assuming that time profiles of the primary and secondary X-ray emissions are similar to those of the primary and secondary microwave emissions. Time variation of the power-law index of the hard X-ray spectrum (30 - 100 keV) is also shown in (c). The Hα data were obtained from the Palehua Observatory patrol film.

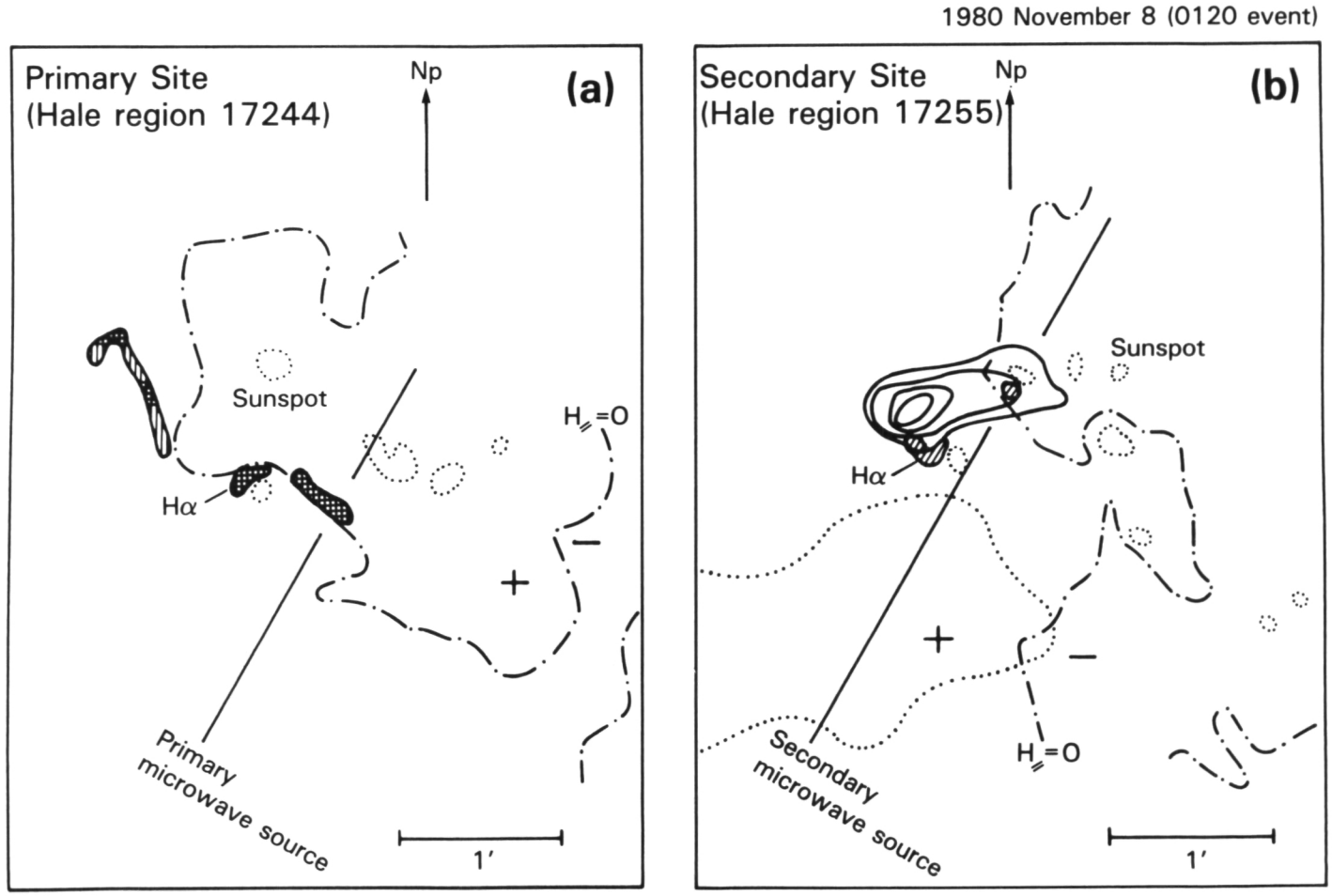

Figure 5. (a) Spatial relationship of the Hα flare (hatched area), the microwave burst at 17 GHz, the magnetic neutral line (dot-dashed line), and the sunspots (dotted-line) for the primary site of the 0120 event on 1980 November 8.

(b) Spatial relationship of the soft X-ray images (01:19-01:20 UT; 3.5-30 keV), the microwave source at 17 GHz, the magnetic neutral line (dot-dashed line), the faint Hα brightenings (hatched area), and the sunspots (dashed-line) for the secondary site of the same event. The X-ray contours in the central part of figure were obtained from HXIS images. The contours are at 75, 50, 25, and 12.5% of the maximum count. A large X-ray bright area (dotted line) present in the HXIS coarse field of view is probably a gigantic loop to the east.

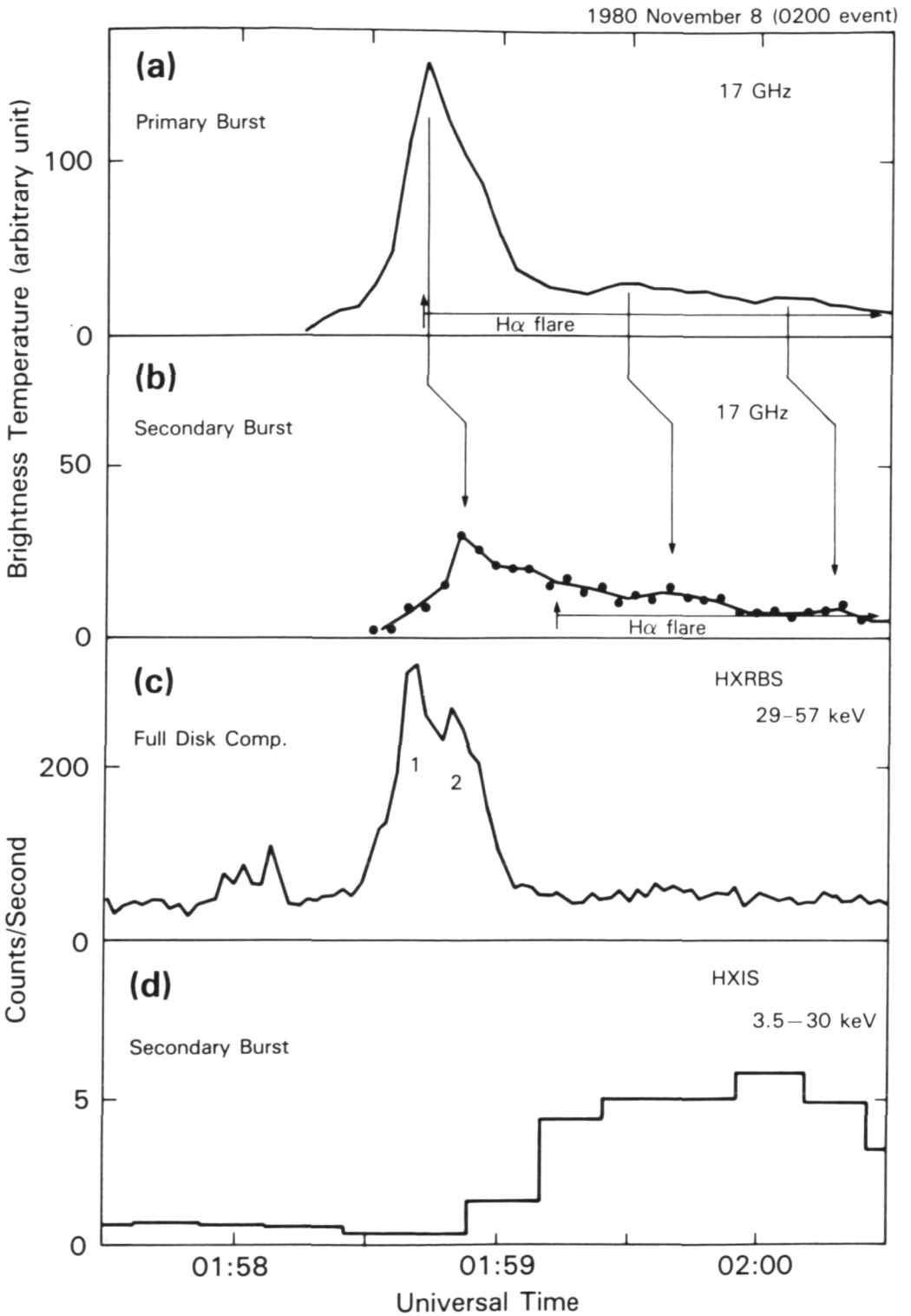

Figure 6. Similar to Figure 4 for the 0200 event on 1980 November 8. Two hard X-ray peaks, 1 and 2, in (c) occur at the same time as the primary and secondary microwave peaks, respectively.

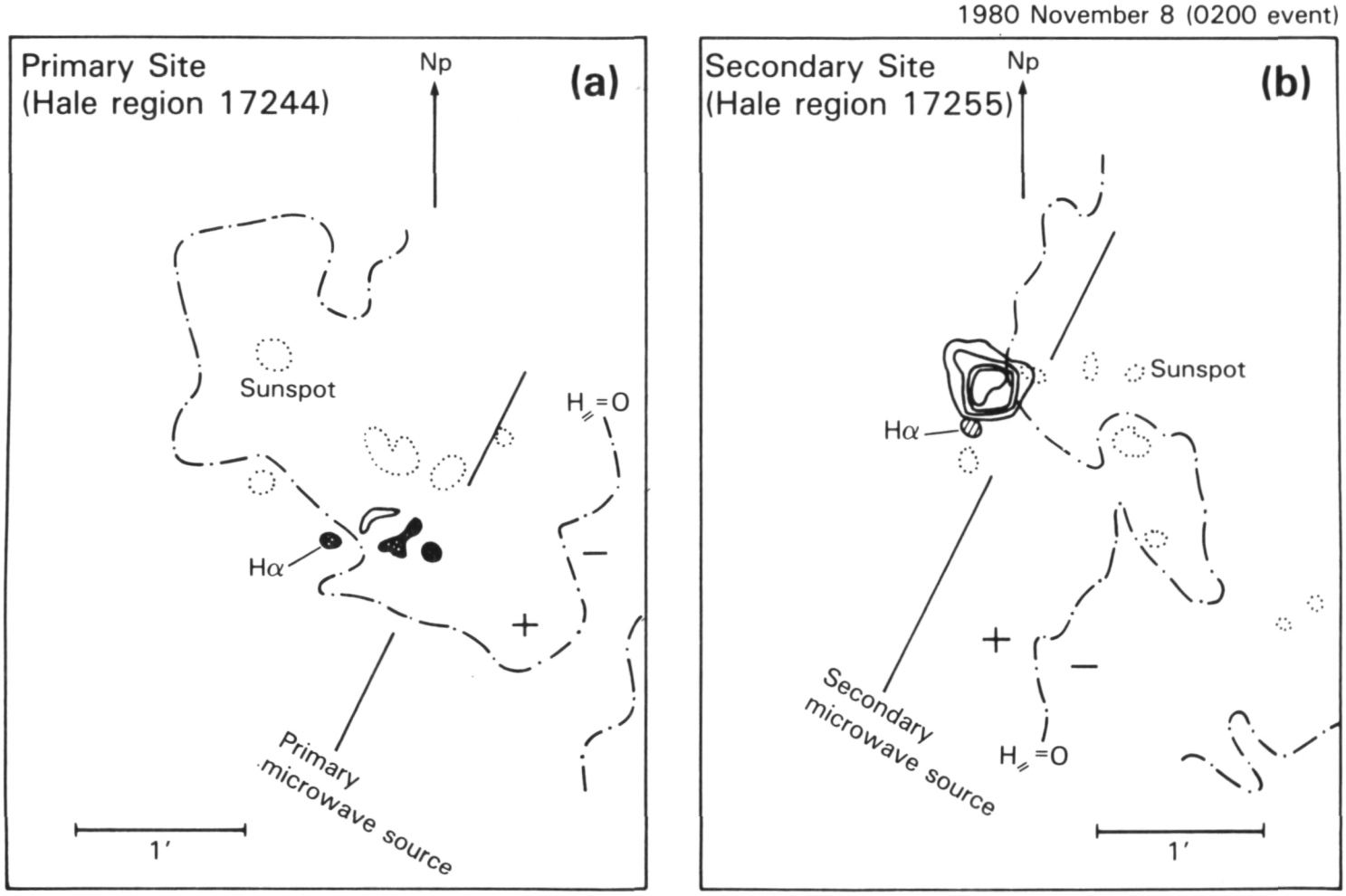

Figure 7. Similar to Figure 5 covering the same area.
(a) Spatial relationship of the Hα flare, the microwave burst at 17 GHz, the magnetic neutral line, and the sunspots, for the primary site of the 0200 event on 1980 November 8.

(b) Spatial relationship of soft X-ray images (01:59-02:01 UT; 3.5-30 keV), the microwave source at 17 GHz, the magnetic neutral line, the Hα brightening, and the sunspots for the secondary site of the same event. The gigantic loop extending to the east limb is omitted.

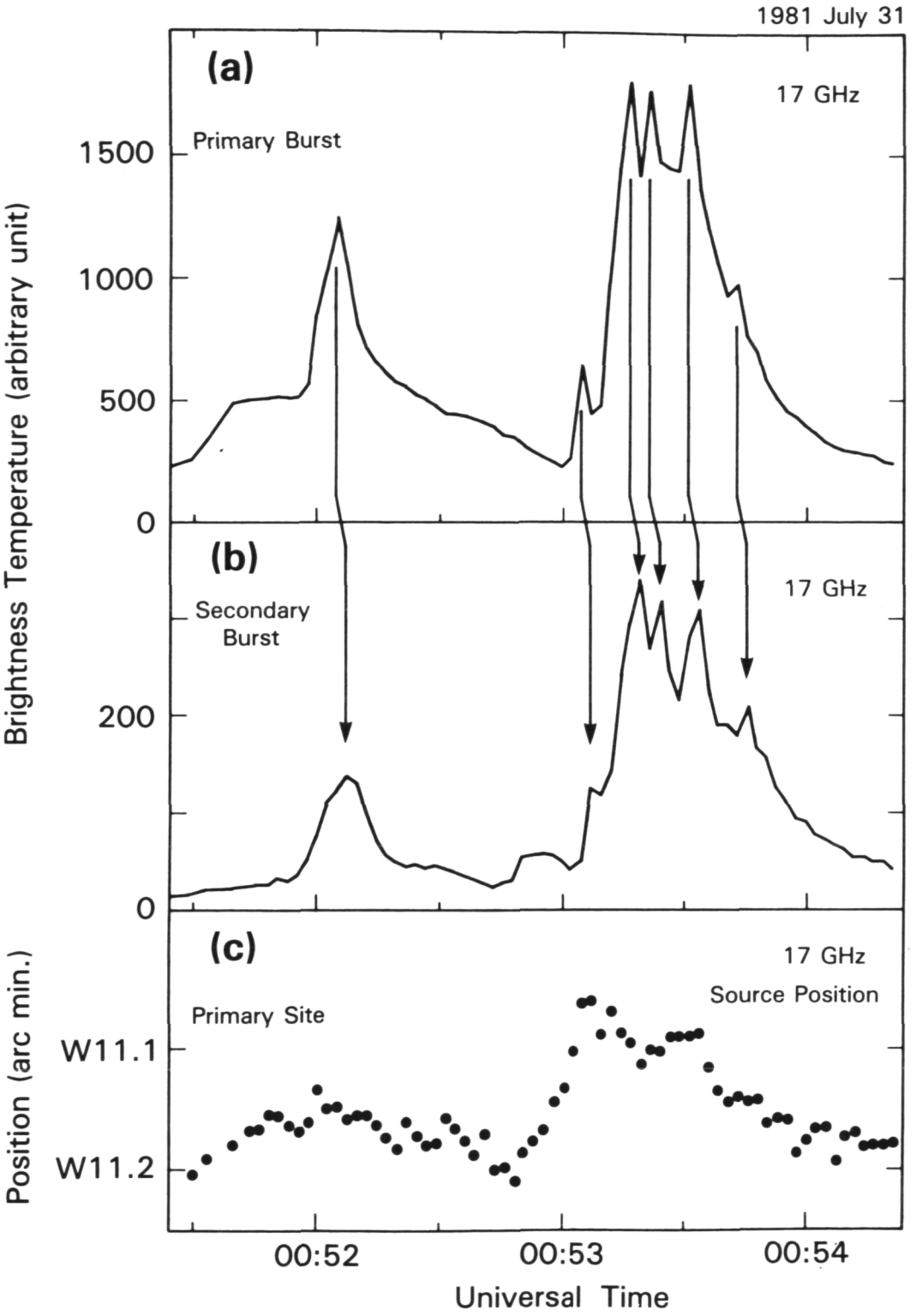

Figure 8. Time variations of the peak brightness temperature of the primary and secondary microwave bursts on 1981 July 31. Arrows indicate well-defined peaks in the primary burst that appear to correspond to delayed peaks in the secondary burst.

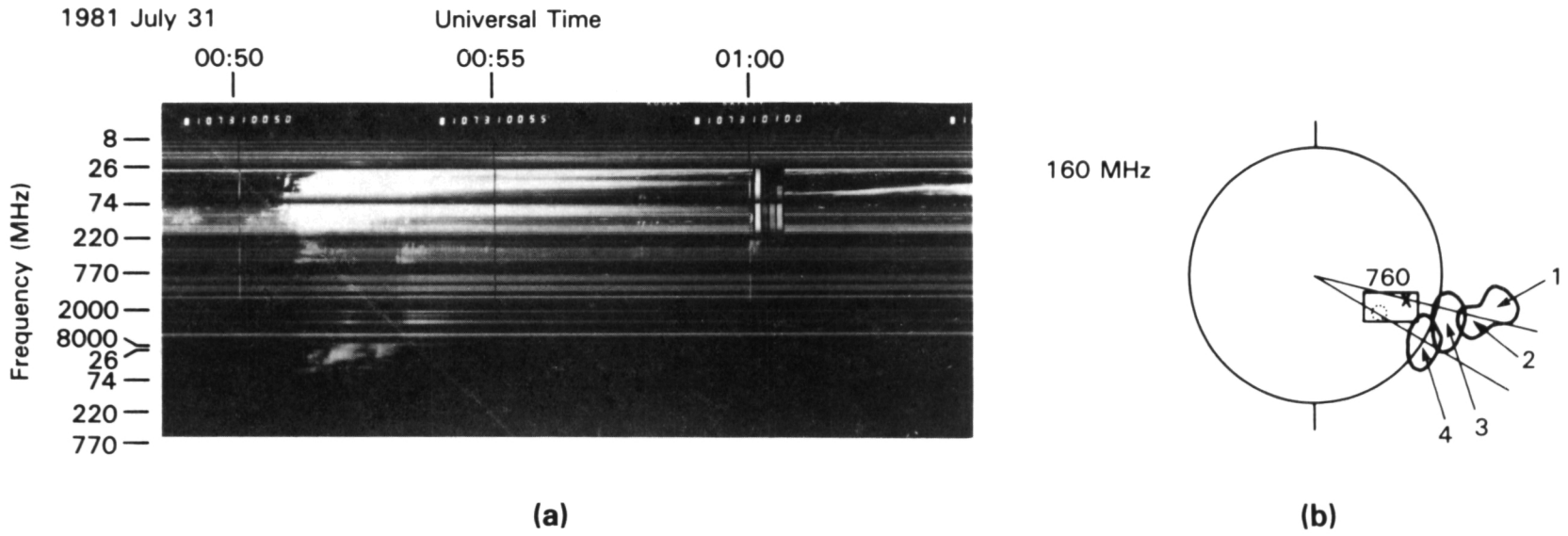

Figure 9. Similar to Figure 3 showing the radio data from Culgoora Solar Observatory for the 1981 July 31 event. The 160 MHz radio heliograph images show the contours of the double type III/V sources at the following times: 00:51:00 (sources 1 and 2), 00:51:57 (1 and 3), 00:53:06 (1 and 4). The two radial lines are drawn through the primary Hα site marked with an 'X' and the sunspot group (dotted circle) which is a candidate for the secondary microwave site.

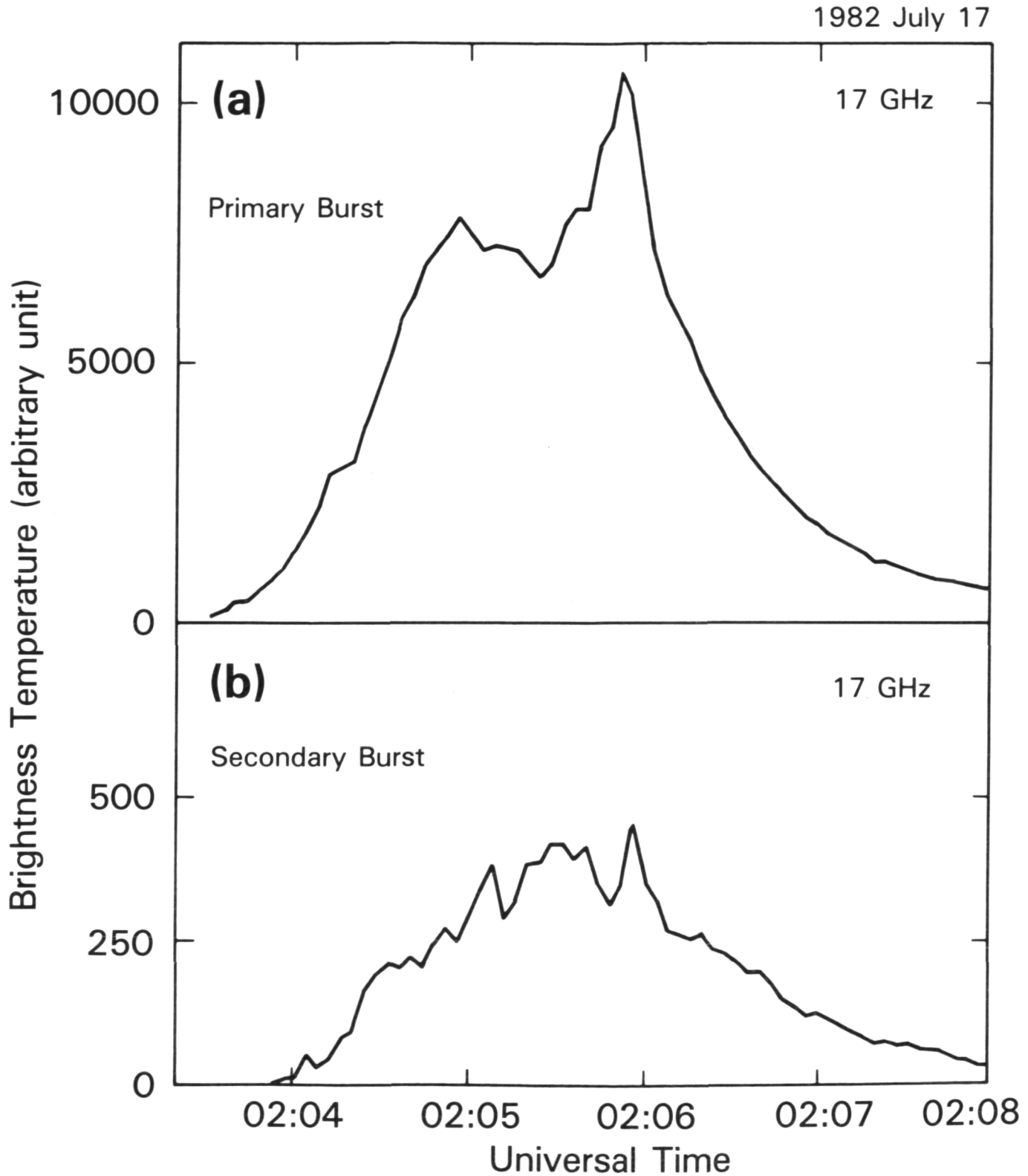

Figure 10. Time variations of the peak brightness temperature of the primary and secondary microwave bursts on 1982 July 17.

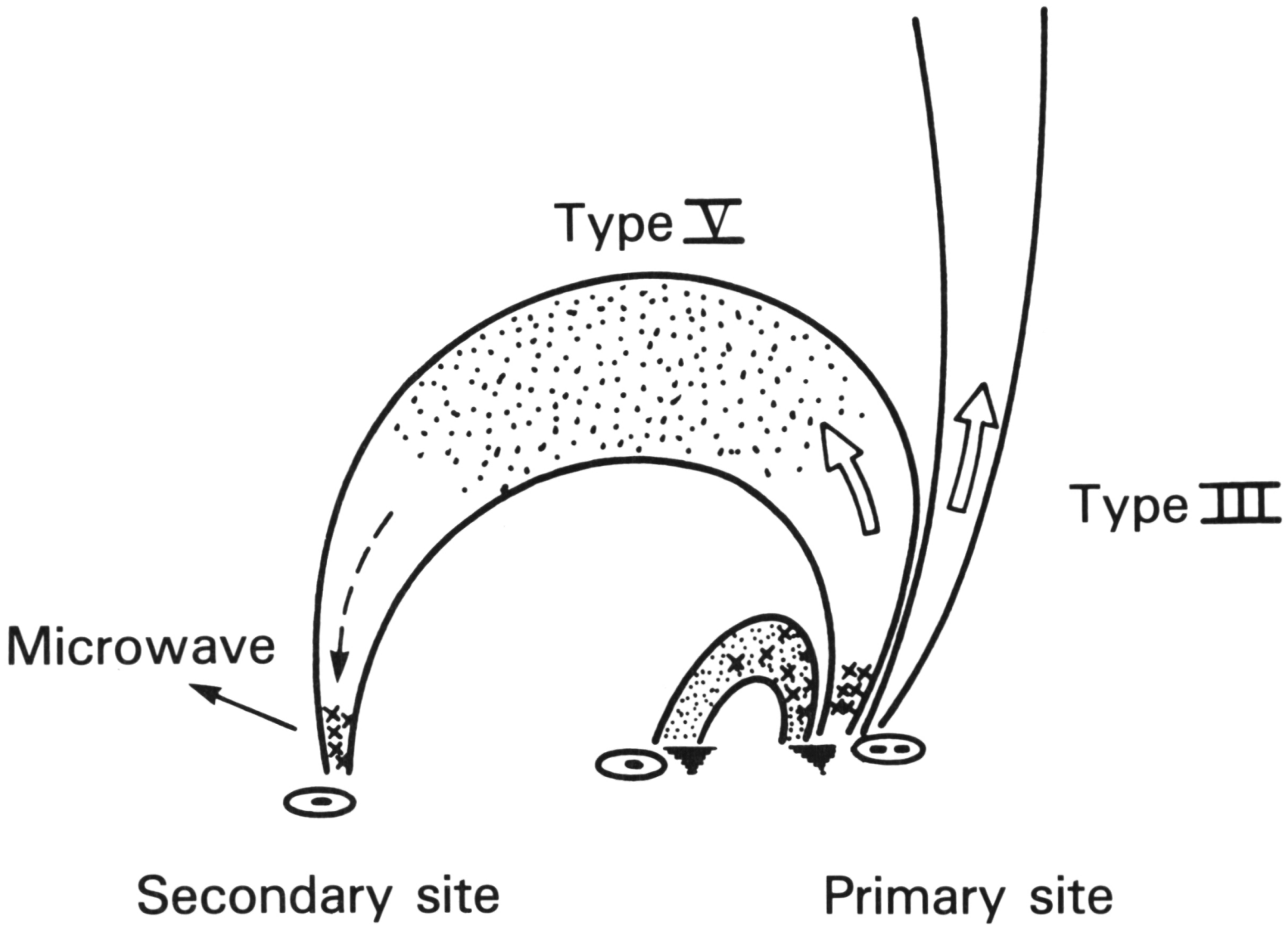

Figure 11. Schematic model of a double microwave burst. Most of the high energy electrons escaping from the primary site towards the secondary site along the huge loop are trapped around the top part of the loop and produce the type V radio burst. The remaining electrons precipitate into the secondary site producing the microwave burst in the low corona. The time profile of the secondary microwave burst is similar to that of the primary burst.

Postal Address

B.R. Dennis and H. Nakajima

Laboratory for Astronomy and Solar Physics

Code 682

Goddard Space Flight Center

Greenbelt, MD 20771

P. Hoyng

Laboratory for Space Research

Beneluxlaan 21,

3527 HS Utrecht

The Netherlands

K. Kai and T. Kosugi

Nobeyama Solar Radio Observatory

Minamisaku-gun

Nagano-ken 384-13

Japan

G. Nelson

CSIRO Solar Observatory

P.O. Box 94

Narrabi, NSW 2390

AUSTRALIA

BIBLIOGRAPHIC DATA SHEET

1. Report No.	2. Government Accession No.	3. Recipient's Catalog No.

4. Title and Subtitle	5. Report Date
Microwave and X-Ray Observations of Delayed Brightenings at Sites Remote From the Primary Flare Locations	August 1984
	6. Performing Organization Code 682
7. Author(s) H. Nakajima, B. R. Dennis, P. Hoyng, G. Nelson, T. Kosugi and K. Kai	8. Performing Organization Report No.
9. Performing Organization Name and Address Laboratory for Astronomy and Solar Physics NASA/Goddard Space Flight Center Greenbelt, MD 20771	10. Work Unit No.
	11. Contract or Grant No.
	13. Type of Report and Period Covered
12. Sponsoring Agency Name and Address	
	14. Sponsoring Agency Code

15. Supplementary Notes

To be published in the Astrophysical Journal

16. Abstract

We present five examples of solar flares observed with the 17-GHz interferometer at Nobeyama in which a secondary microwave burst occurred at a distance of 10^5 to 10^6 km from the primary flare site. The secondary microwave burst in all five cases had a similar time profile to the primary burst with a delay of 2 to 25 s. The velocity of a triggering agent inferred from this delay and spatial separation is 10^4 - 10^5 km s^{-1}. The intensity of the secondary burst was a factor of 3 to 25 smaller than that of the primary burst in all events except for one case in which it was a factor of 2 larger. The polarization degree of the secondary burst at 17 GHz was >35%, significantly higher than the average value for typical impulsive bursts. Two of the events were accompanied by meterwave type III/V bursts located high in the corona between the primary and secondary sites. For two of the other events, X-ray images of the secondary source were obtained with the Hard-X-Ray Imaging Spectrometer on the Solar Maximum Mission. These observations strongly suggest that the distant microwave bursts were produced by electrons with energies of 10 to 100 keV which were channeled along a huge loop from the main flare site to the remote location.

17. Key Words (Selected by Author(s))	18. Distribution Statement
Remote Brightenings, Microwaves, X-Rays, Solar Flares	

19. Security Classif. (of this report)	20. Security Classif. (of this page)	21. No. of Pages	22. Price*
Unclassified	Unclassified	37	

*For sale by the National Technical Information Service, Springfield, Virginia 22151.